Laser and Particle Beams (2012), *30*, 183–188.

doi:10.1017/S0263034611000796

2D analysis of direct-drive shock-ignited HiPER-like target implosions with the full laser megajoule

B. CANAUD,[1] S. LAFFITE,[1] V. BRANDON,[1] AND M. TEMPORAL[2]
[1]CEA, DAM, DIF, F-91297 Arpajon, France
[2]Universidad Politécnica de Madrid, 28040 Madrid, Spain

(RECEIVED 25 July 2011; ACCEPTED 29 August 2011)

Abstract

We present a 2D analysis of direct-drive shock ignition for the laser Megajoule. First, a target design is chosen in the HiPER-like target family generated by scale up and down of the original HiPER target. A first analysis is done considering the 1D fuel assembly and 2D shock ignition by means of the ring at polar angle of 33°2. The intensity profile is top-hat and calculations are done for several different radii. It is shown that larger the radius, lower the minimum spike power is. In addition, the intensity in each quad can stay below 4×10^{14} W/cm^2 and is considered non crucial for parametric instabilities such as two plasmons. A 2D analysis of the fuel assembly is done in a second step by considering the two rings located at 49° and 59°5 and their symmetric by the equatorial plane symmetry. It is shown that low mode asymmetries are important at the stagnation and can significantly affect the areal density obtained. Finally, full 2D calculations of shock ignition is done, using all the beams of the LMJ and show that the spike power needed for ignition and gain is increased by a factor greater than 3 regarding the power needed in perfectly isotropic fuel assembly. This increase is mainly due to high level low mode asymmetries generated during fuel assembly.

Keywords: Direct-Drive fusion; Inertial confinement fusion; Shock Ignition

1. INTRODUCTION

Conventional high gain direct-drive fusion studies for the laser megajoule (LMJ) consider self-igniting target design with the direct-drive beam irradiation geometry (Canaud *et al.*, 2002, 2004*a*) or with the X-ray drive geometry (Canaud *et al.*, 2007*a*, 2007*b*) without or with zooming (Canaud *et al.*, 2005; Temporal *et al.*, 2010). In addition, the capability of direct-drive self-ignition of LMJ indirect-drive beam geometry has been demonstrated (Canaud *et al.*, 2007*a*) with zooming due to the specificity of the beam layout of LMJ leading to the surrender of the specific direct-drive beam layout. Polar direct drive (Canaud *et al.*, 2004*b*) was not necessary to achieve direct-drive high thermonuclear gain with LMJ as long as the LMJ would have all the indirect drive beams. The condition to achieve high gain obliged to use zooming which introduces an additional constraint for the facility. Indeed, without zooming, the target is marginally igniting due to the low level of laser energy of 1 MJ with two rings. In complementary to cryogenic DT implosion, which requires the employment of cryogenic system (Perin, 2010), direct-drive implosion of double shell targets (Canaud *et al.*, 2011) is considered for moderate thermonuclear gain.

Recently, direct-drive shock ignition of HiPER-like target (Canaud *et al.*, 2010) was addressed for LMJ in 1D-calculations. The use of strong convergent shock waves was first proposed by Betti (2007) in order to ignite targets and was considered to match the LMJ requirements. Results (Canaud *et al.*, 2010) show that shock ignition of a non-igniting target, well below its self-ignition threshold, is easier to do when the target is close to the threshold. This renewal of shock waves interest in inertial confinement fusion comes from the applications that can be done in fusion energy (Eliezer *et al.*, 2011). In order to generate the ignitor shock wave, Betti proposed to use an additional laser spike with a power and a start-time adjusted to the target design. As far below from its self-ignition threshold the target is, as high the spike power has to be. In contrast, the nearest

Address correspondence and reprint requests to: B. Canaud, CEA, DAM, DIF, F-91297, Arpajon, France. E-mail: benoit.canaud@cea.fr

to the threshold the target is, the lowest the spike power is. In this case, the energy needed for fuel assembly becomes higher when considering targets increasingly close to their threshold.

All previous calculations for LMJ were mono-dimensional. In this paper, we address a 2D analysis of direct-drive shock ignition for a HiPER like target which is a compromise between fuel assembly energy and ignitor spike power in agreement with the LMJ specifications.

Historically, LMJ indirect drive irradiation consists in 60 beams (quadruplets or quads) distributed on three rings per hemisphere as shown on Figure 1. Specificity of this beam layout is that beams at polar angles of 49° and 59°5 are located on both sides of the Schmitt angle (Schmitt, 1984): $\theta_0 = 54.736°$. Ring-to-ring power balance τ_k has to satisfy $\sum_k \tau_k(\cos(2\theta_k) + 1/3) = 0$. Using the Schmitt rules completed by $\sum_k \tau_k = 1$, the best solution for direct drive is to use both rings at polar angle of 49° and 59.5° with a ring-to-ring balance of $\tau_{49°} = 0.78$ and $\tau_{59.5°} = 1$. In this case, cones at polar angles of 49° and 59.5° should deliver 45% and 55% of the total energy, respectively. Finally, the facility should deliver only 1 MJ due to the energy limitation (to 300 kJ per cone) in each cone. Beams at the polar angle of 33°2 are unemployed and could be used for shock ignition.

In a two-step study, we analyze the possibility of direct-drive shock ignition with LMJ, using both rings at 49° and 59°5 for fuel assembly and the ring at 33°2 for ignition. The first step consists in looking at the effect of the 33°2-ring. The fuel assembly is done in 1D dimension and the ignition is done with a spike launched by the ring at 33°2 with a top-hat intensity profile. Different focal spot diameters are analyzed. The second step consists in doing calculation with the full LMJ.

The numerical calculations are performed with the 2D Lagrangian radiation-hydrodynamics code FCI2 (Buresi, 1986). It includes tabulated equations of state (i.e., SESAME), flux-limited Spitzer heat transport, multigroup radiative transfer, 1D or 2D ray-tracing, multigroup alpha particle transport, and neutron transport.

The target considered here is an all-DT HiPER-like target (Canaud *et al.*, 2010) described in Figure 1 and obtained by a scale up of the initial HiPER target (Atzeni, 2009). The external radius is 1560 μm and the DT ice thickness is 316 μm. The 1D-laser pulse, also described in Figure 1, drives the 1D-implosion on a low in-flight adiabat (defined as the ratio of the multiple-shock induced-pressure over the Fermi pressure: $\alpha = P[MPa]/2.17\rho^{5/3}$ [kg/m^3] ~0.8) at a peak implosion velocity of 290 km/s. At stagnation, the peak areal density is $\rho r \sim 19$ kg/m^2 and peak density is $\rho \sim 680 \times 10^3$ kg/m^3.

2. 1D FUEL ASSEMBLY AND 2D SHOCK IGNITION

In a first step, we consider 1D-calculation of the fuel assembly with 1D-centered laser beams and an additional laser beam located at a polar angle of 33°2 in order to create the ignitor shock by a laser spike. In calculations, this last laser beam is modelized by 3D-ray tracing algorithm. The focal shape is top-hat circular intensity profile with a radius r_0 varying from 0.8 to 1.2 mm. The spike is a 300 ps long flat laser pulse with 200 ps rise and fall times. A variation of spike power P_{spike} and pulse timing between driver and spike is performed to find the ignition window.

Figure 2 shows the thermonuclear gain versus the spike power. The thermonuclear gain is defined by: $G = E_{th}/(E_{1D}/\eta_{3D} + E_{spike})$ where E_{1D}, η_{3D}, and E_{spike} are the 1D-fuel assembly drive energy, the laser-target coupling efficiency η_{3D} and the ignitor spike energy respectively. η_{3D} is defined as the ratio of the absorbed energy divided by the incident 3D-energy. This ratio is roughly estimated at 0.5 by looking at all previous simulations (Canaud *et al.*, 2004*a*, 2005, 2007*a*) of direct-drive implosion done in 2D-calculation by means of FCI2. As it can be seen, smaller the focal spot, better the laser-target coupling is, and lower the ignitor spike power has to be. The spike time of launch is late in the implosion, typically, during the second half part of the main drive. Usually, the plasma blow off pushes

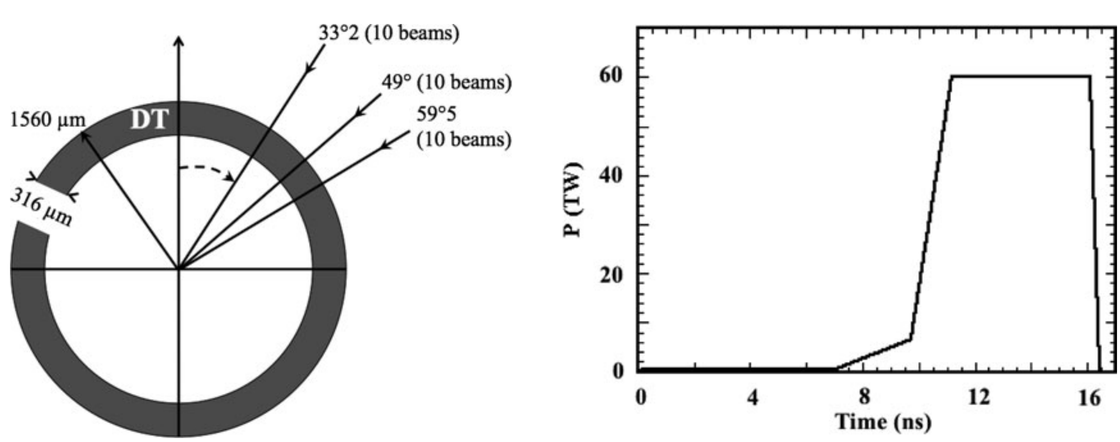

Fig. 1. HiPER-like target design, beam layout around the target for indirect drive and laser pulse.

https://doi.org/10.1017/S0263034611000796 Published online by Cambridge University Press

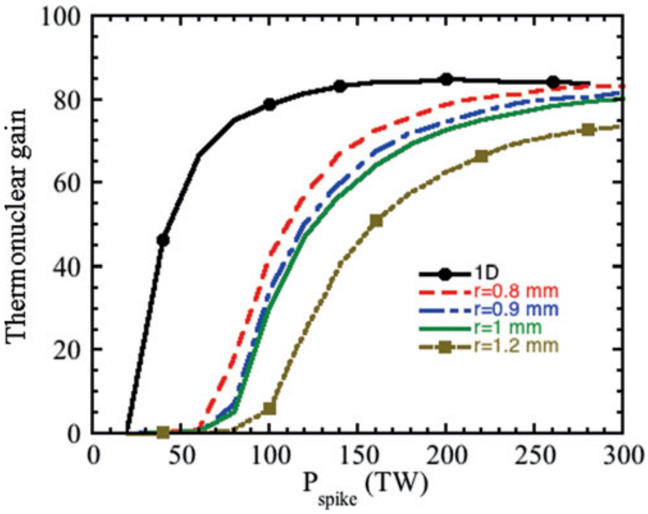

Fig. 2. (Color online) Thermonuclear gain versus the spike power for the ring at 33°2 for three different focal spot radii (0.8 mm: dashed line, 0.9 mm: dot-dashed-line, 1 mm: plain line, and 1.2 mm: dotted line and squares) compared the full-1D calculation (plain line and circles).

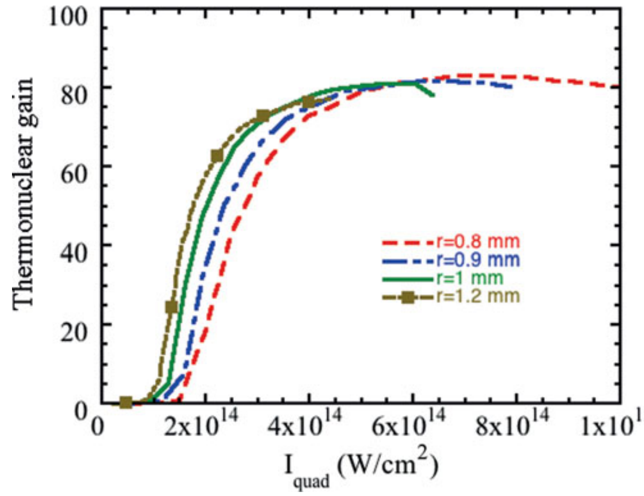

Fig. 3. (Color online) Thermonuclear gain versus the spike intensity of each quad of the ring at 33°2 for three different focal spot radii (0.8 mm: dot-dashed line, 0.9 mm: dotted-line, and 1 mm: plain line).

the plume far from the ablation front. Even if the critical density radius decreases in time, the quarter-critical density stays at the same radius, at roughly 1.2 mm in our case.

In conventional direct-drive, the drive intensity is sufficiently at a low level to neglect parametric instability such as two plasmons decay. This last takes place mainly at the quarter-critical density and is deleterious for implosion due to mainly suprathermal electrons. The intensity threshold for two plasmon instability is usually given (Simon *et al.*, 1983) by: I_{14} [W/cm^2] $\sim 80 T_e$ [*keV*]/λ [μm]/L[μm] where T_e, λ, and L stand for the electronic temperature (in keV), the laser wavelength in vacuum (in μm), and the plasma scale-length ($L = n_e/\nabla n_e$, in μm), respectively. In our simulations, during the spike temporal window, electronic temperature evolves from 2.5 keV without spike to 3.5 keV with spike while the density scale length decreases from 300 μm without spike to 200 μm with spike. With this hydrodynamics conditions, the two plasmon instability threshold is about 3×10^{14} W/cm^2. For shock ignition of the HiPER target, the spike intensity could be at very high level well above 10^{15} W/cm^2. In our case, the target is bigger than the HiPER target. Its distance to the self-ignition threshold is much smaller than the one of the HiPER target and the power required to shock ignition is also smaller as shown in Canaud *et al.* (2010). As the ignitor focal spot radius is larger, the ignitor shock is much more isotropic and ignition requires less power in the spike to achieve ignition and gain. In addition, the increase of the radius leads to a quadratic reduction of the intensity needed to ignite the target. Finally, Figure 3 shows the thermonuclear gain versus the intensity in each quad. It seems relevant to assume that, at each point located at the quarter-critical radius, only few quads of the ring at 33°2 overlap. The laser refraction is assumed to mismatch the phase of the laser field. The interaction of quads, one with the others, is supposed to be non-coherent, thus no constructive. Under these assumptions, each quad can be considered independently. From Figure 3, it can be seen that the intensity in each quad is at a low level of few 10^{14} W/cm^2. However, this intensity is superimposed to the fuel assembly intensity which is about 2×10^{14} W/cm^2. Nevertheless, the resulting intensity stays at low level, well below 10^{15} W/cm^2. These results show that to choose a target design not so far from the self-ignition threshold allows to reduce the intensity of the ignitor spike at level of the order of two-plasmon decay threshold.

3. 2D FUEL ASSEMBLY

In this section, we consider the fuel assembly done by using two rings located at polar angles of 49° and 59°5, respectively. By the past, we have shown in Canaud *et al.* (2007*a*) that this beam geometry meets the Schmitt (1984) requirements. However, the Schmitt calculations assumed that the absorbed intensity is a cos^2 (θ)-law. In order to estimate a more realistic estimate of the root-mean-square (rms) deviation of the intensity uniformity, a full 3D-ray tracing algorithm has been developed (Temporal and Canaud, 2009) and used to propose a detailed analysis of the HiPER irradiation geometry (Temporal *et al.*, 2010). This tool uses as input, hydrodynamics data such as density, temperature time-resolved radial profiles given by 1D hydrodynamics simulation of the implosion of a target. A remapping is done over a full sphere and 3D ray-tracing algorithm allows to deal with refraction and energy deposition by inverse Bremsstrahlung along ray paths.

We use this tool to estimate the root mean square (rms) deviation of the absorbed intensity (and not the incident or direct illumination) given by this full 3D-ray-tracing tool and produced

https://doi.org/10.1017/S0263034611000796 Published online by Cambridge University Press

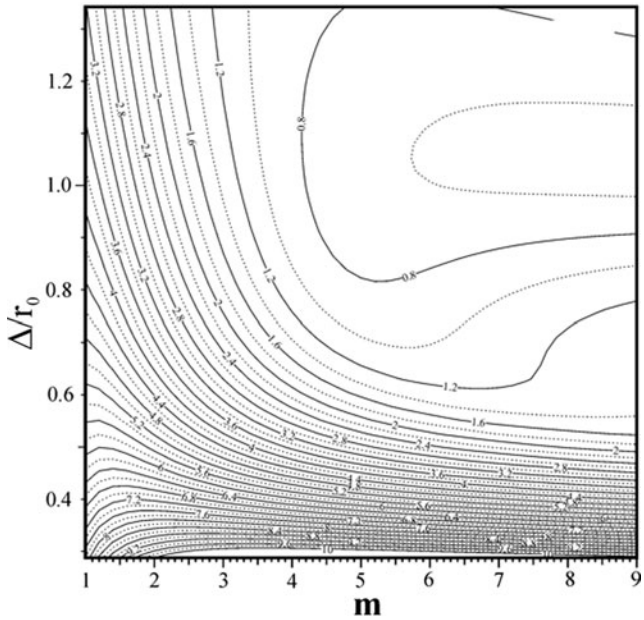

Fig. 4. Isovalues of the rms deviation for the absorption uniformity versus both supergaussian parameters m and Δ.

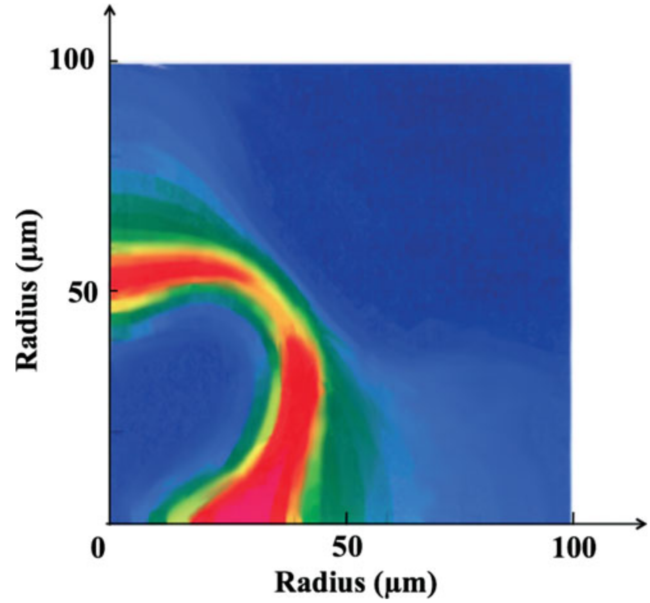

Fig. 5. (Color online) 2D image of the density at stagnation of a HiPER-like target illuminated by the two-rings geometry of LMJ. Beams are equally distributed on azimuth at two polar angles of 49° and 59°5, and their symmetric by the equatorial plane symmetry.

by the two-rings LMJ geometry. The intensity profile is assumed to be a supergaussian function of the transverse coordinate: $\exp(-(x/\Delta)^m)$ where Δ is the half-width at $1/e$ and m the slope. The rms-deviation σ is given in Figure 4 during the main drive.

We can see that during the drive part, the minimum non-uniformity is achieved for large top-hat focal spot. In this calculations, the ring-to-ring power imbalance is 1:1. We used these input data in 2D-calculations of the implosion done with FCI2 using the 3D-ray tracing package. Calculations used a top-hat intensity profile, a focal spot radius equal to $0.9 \times r_{target} = 940$ µm, and the same laser power for beams at polar angle of 49° and 59°5. The laser pulse is reshaped in comparison to the 1D-pulse in order to take into account the 3D aspect of the laser beams (especially, the energy losses by the side of the imploding target). Zooming is not considered here. The modified laser pulses show an increase of the drive power by a factor 3 and the incident energy changes from 360 kJ in 1D to 850 kJ in FCI2. The laser-target efficiency η_{3D} is 0.56, close to the estimate done previously.

The residual low mode asymmetries of this irradiation geometry are fully seen on the 2D map of the density at the stagnation, as shown in Figure 5. A significant contribution of modes 2 and 4 in the Legendre expansion representation can be observed in this figure with a peak-to-valley of roughly 35% and 15%, respectively.

The implosion velocity and the in-flight adiabat are kept similar to the 1D ones. However, a reduction of the peak density and areal density is observed due to the anisotropy of the stagnating shell. Indeed, the areal density changes from 18.5 kg/m^3 to 16 kg/m^2 with a rms deviation of 37%. These low mode asymmetries have been observed in the past (Canaud *et al.*, 2007*a*) for baseline direct-drive target design with the indirect-drive beam layout.

Losses by the side of the imploding target are very important and zooming technique should improve significantly the laser-target coupling efficiency. But zooming can also improve the absorption uniformity during the drive part (Canaud *et al.*, 2005, 2007*a*; Temporal *et al.*, 2010). This option should be done on LMJ by using differently beams in each ring. Indeed, each ring has 10 beams. A first part of the laser pulse, and thus the implosion history, can be achieved using only five beams per ring. Then the drive part is done using the last five beam per ring with an adapted intensity profile. Another possibility to improve the irradiation uniformity of the fuel assembly consists in using non-equal ring-to-ring power imbalance between the ring at 49° and 59°5. Finally, the last option should be to optimize separately intensity profiles for each ring.

Mixing these different options should reduce significantly the absorption non-uniformity and reduces by this way the low mode asymmetries at stagnation.

4. FULL 2D CALCULATIONS: 2D FUEL ASSEMBLY AND 2D SHOCK IGNITION

Using the previously described beam geometry for fuel assembly and shock ignition, we performed 2D calculation of the whole implosion and ignition.

The fuel assembly is achieved with beams that have the same parameters than in the previous section: beams are located at polar angles of 49°, 59°5, 120°5, and 131°. They

https://doi.org/10.1017/S0263034611000796 Published online by Cambridge University Press

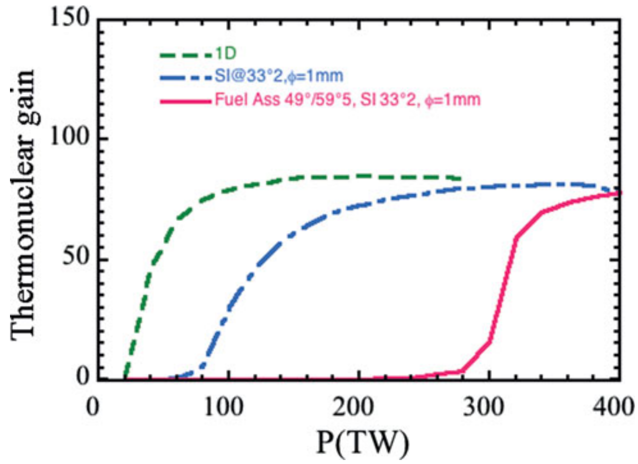

Fig. 6. (Color online) Thermonuclear gain versus the spike power for full-1D calculation (dashed line), for 1D-full assembly and shock ignition at 33°2 (dot-dashed line), and for full 2D calculation (2D full assembly and 2D shock ignition, plain line).

have the same top-hat intensity profile with a radius of $0.9r_0$, where $r_0 = 1560$ μm is the initial radius of the target.

Shock ignition is done by the use of beams located at polar angle of 33°2 and 147°8 with a top-hat intensity profile and a radius of 1 mm. A variation of spike time of launch and power is done in order to achieve high thermonuclear gain. Figure 6 shows a comparison of shock ignition for the full-1D calculations, for 1D-full assembly and 2D shock ignition, and for the full 2D calculations. It can be seen that high thermonuclear gain is achieved for higher spike power in full 2D-calculations. This power increase is mainly due to strong low mode asymmetries observed at stagnation due to the full assembly done in a quasi-direct drive beam geometry. This beam layout has a strong consequence on self-ignition threshold and displaces it towards higher energies as observed previously (Canaud *et al.*, 2007*a*) in the baseline direct-drive target design. As the self-ignition threshold is at higher level, the power need to reduce it by shock ignition is more important.

The use of zooming technique and an optimization of the absorption uniformity should improve significantly the uniformity of the implosion and reduce the power need to shock ignite the target by reducing the 2D self-ignition threshold.

5. SUMMARY

In this paper, we present a 2D analysis of direct-drive shock ignition for the laser Megajoule. First, a target design is chosen in the HiPER-like target family generated by scale up and down of the original HiPER target. A first analysis is done considering the 1D fuel assembly and 2D shock ignition by mean of the ring at polar angle of 33°2. The intensity profile is top-hat and calculations are done for different radii. It is shown that smaller the radius, lower the spike power is. In addition, the intensity in each quad can stay below 4×10^{14} W/cm^2 and is considered non crucial for parametric instabilities such as two plasmons. A 2D analysis of the fuel assembly is done in a second hand by considering the two rings located at 49° and 59°5 and their symmetric by the equatorial plane symmetry. It is shown that low mode asymmetries are important at the stagnation and can significantly affect the areal density obtained. In addition, the drive part being long, the laser-target coupling efficiency is at low level (56%). Finally, full 2D calculations of shock ignition is done, using all the beams of the LMJ and show that the spike power needed for ignition and gain is increased by a factor greater than 3 regarding the power needed inperfectly isotropic fuel assembly. This increase is mainly due to high level low mode asymmetries generated during fuel assembly.

To conclude, a special attention will be paid in the future to improve significantly the fuel assembly isotropy by reducing the target aspect ratio and the laser-target coupling efficiency by mixing zooming technic, new target redesign with short drive duration, and ablator providing better absorption rate than pure DT.

ACKNOWLEDGMENTS

M.T. was supported by the research contract n°. 2007-00447 of the Spanish Ministry of Education and Research.

REFERENCES

Atzeni, S. (2009). Laser driven inertial fusion: The physical basis of current and recently proposed ignition experiments. *Plasma Phys. Contr. Fusion* **51**, 124029.

Betti, R., Zhou, C.D., Anderson, K., Perkins, L.J., Theobald, W. & Solodov, A.A. (2007). Shock ignition of thermonuclear fuel with high areal density. *Phys. Rev. Lett*. **98**, 155001.

Buresi, E., Coutant, J. & Dautray, R. (1986). Laser program-development at CEL-V: Overview of recent experimental results. *Laser Part. Beam* **4**, 531.

Canaud, B. & Garaude, F. (2005). Optimization of laser-target coupling efficiency for direct drive laser fusion. *Nucl. Fusion* **45**, L43.

Canaud, B. & Temporal, M. (2010). High-gain shock ignition of direct-drive ICF targets for the laser megajoule. *New J. Phys.* **12**, 043037.

Canaud, B., Fortin, X., Dague, N. & Bocher, J.L. (2002). Laser megajoule irradiation uniformity for direct drive. *Phys. Plasmas* **9**, 4252.

Canaud, B., Fortin, X., Garaude, F., Meyer, C. & Philippe, F. (2004*a*). Progress in direct-drive fusion studies for the laser megajoule. *Laser Part. Beam* **22**, 109.

Canaud, B., Fortin, X., Garaude, F., Meyer, C., Philippe, F., Temporal, M., Atzeni, S. & Schiavi, A. (2004*b*). High gain direct-drive target design for the laser megajoule. *Nucl. Fusion* **44**, 1118.

Canaud, B., Garaude, F., Ballereau, P., Bourgade, J.L., Clique, C., Dureau, D., Houry, M., Jaouen, S., Jourdren, H., Lecler, N., Masse, L., Masson, A., Quach, R., Piron, R., Riz, D., Van der Vliet, J., Temporal, M., Delettrez, J.A. & McKenty, P.W. (2007*a*). High-gain direct-drive inertial confinement fusion for the laser meajoule: Recent progress. *Plasma Phys. Contr. Fusion* **49**, B601.

Canaud, B., Garaude, F., Clique, C., Lecler, N., Masson, A., Quach, R. & Van der Vliet, J. (2007*b*). High-gain direct-drive laser fusion with indirect drive beam layout of laser megajoule. *Nucl. Fusion* **47**, 1652.

Canaud, B., Lafte, S. & Temporal, M. (2011). Shock ignition of direct-drive double-shell targets. *Nucl. Fusion* **51**, 062001.

Eliezer, S. & Martinez Val, J.M. (2011). The comeback of shock waves in inertial fusion energy. *Laser Part. Beam* **29**, 175.

Perin, J.P. (2010). Cryogenic systems for LMJ cryotarget and HiPER application. *Laser Part. Beam* **28**, 203.

Schmitt, A.J. (1984). Absolutely uniform illumination of laser fusion pellets. *Appl. Phys. Lett*. **44**, 399.

Simon, A., Short, R.W., Williams, E.A. & Dewandre, T. (1983). On the inhomogeneous two-plasmon instability. *Phys. Fluids* **26**, 3107.

Temporal, M & Canaud, B. (2009). Numerical analysis of the irradiation uniformity of a directly driven inertial confinement fusion capsule. *Eur. Phys. J. D* **55**, 139.

Temporal, M., Canaud, B. & LeGarrec, B.J. (2010). Irradiation uniformity and zooming performances for a capsule directly driven by a 32×9 laser beams configuration. *Phys. Plasmas* **17**, 022701.

Temporal, M., Canaud, B., Lafte, S., LeGarrec, B.J. & Murakami, M. (2010). Illumination uniformity of a capsule directly driven by a laser facility with 32 or 48 directions of irradiation. *Phys. Plasmas* **17**, 06504.